Materials Advances

Accepted Manuscript

This article can be cited before page numbers have been issued, to do this please use: R. Ferraiuolo, C. Carandente Coscia, R. Esposito, M. G. Maglione, P. Tassini, G. Vitiello, G. D'Errico and A. Pezzella, *Mater. Adv.*, 2024, DOI: 10.1039/D4MA00339J.

View Article Online
DOI: 10.1039/D4MA00339J

Synergistic radical concentration increase in eumelanin-PEDOT:PSS blends: mammalian pigment-based doping for thermopower improvement.

Raffaella Ferraiuolo,[1‡] Carlo Carandente Coscia,[2,3‡] Maria Grazia Maglione,[4,5] Paolo Tassini,[4,5] Rodolfo Esposito,[2,3] Giuseppe Vitiello,[3,6] Gerardino d'Errico,[2,3] Alessandro Pezzella[1,5,7,8 *]

[1] Department of Physics "Ettore Pancini", University of Naples "Federico II", 80126 Naples, Italy;
[2] Dept. of Chemical Science, University of Naples Federico II, Naples, Italy
[3] Consorzio Interuniversitario per lo Sviluppo dei Sistemi a Grande Interfase (CSGI), Via della Lastruccia 3, 50019 Sesto Fiorentino (FI), Italy
[4] Laboratory of Nanomaterials and Devices (SSPT-PROMAS-NANO) ENEA – C. R. Portici P.le E. Fermi 1 Loc. Granatello I-80055 Portici (NA), Italy
[5]Bioelectronics Task Force at University of Naples Federico II, Italy
[6] Dept. of Chemical, Materials and Production Engineering, University of Naples Federico II, Naples (IT)
[7] National Interuniversity Consortium of Materials Science and Technology (INSTM), Piazza S. Marco, 4, 50121 Florence, Italy
[8] Institute for Polymers Composites and Biomaterials (IPCB) CNR Via Campi Flegrei 34, I-80078 Pozzuoli (NA), Italy

Abstract

Moving from previous investigation of eumelanin and PEDOT:PSS blends we devised to explore the possible contribution of eumelanin to termopower improvement of PEODT:PSS in light of the well known radical character of the mammalian pigment. Determination of Seebeck coefficient and conductivity showed effective contribution of eumelanin blending to the PEDOT thermoelectric properties. Notably these effects correlate with a marked modification of paramagnetic features of both PEDOT and eumelanin after blending.

Introduction

View Article Online
DOI: 10.1039/D4MA00339J

The growing diffusion of organic electronic devices is rooted on several factors, from the design and fabrication of new architectures to the development of advanced material tailored for a wide range of applications in optoelectronics[1] or energy storage[2] and sensing[3] just to mention few. Energy conversion also can take advantage on organic materials as, for example, thermoelectric devices based on conducting polymers are promising tools for several applications, chiefly self powered health monitor device[4] and more generally wearable devices which requires conformable substrates.[5] In this scenario valuable thermoelectric conversion carries strict requirements to the electronic structures of the active organic materials whose rational design and precise modulation are producing new state of art TE devices.[6] Indeed, great advancements are emerging by integrating of different conjugated polymers.[7] However, the intrinsic semiconducting nature inherent to the macromolecular architecture of common conjugated polymers requires some doping to rise electrical conductivity as well as to optimize thermoelectric performance.[2] Therefore, the search for new materials (chiefly polymers) featuring tunable properties possibly by doping with easy to handle sustainable additives and by facile protocols is gaining interest in the field of organic electronics and bioelectronics.

In these perspective recent observations suggest that the addition of a tailored open-shell systems significantly increases the Seebeck coefficient ***s*** in a material involving a single species[8] as well as allows for the systematic manipulation of the thermoelectric properties for nontraditional CP thermoelectric systems, resulting in an optimized power factor above 10 $\mu W m^{-1} K^{-2}$, one of the largest values reported.[9] Moreover, a combination of open-shell small molecule dopants and macromolecules bearing stable radical groups is also emerging as a tool to control charge transport, reduce thermal conductivity and enable improved behavior in polymer-based thermoelectric systems.[9, 10]

Eumelanin polymers[11] posses intrinsic radical population[12] featuring whose persistence is consistent with stabilization of unpaired electrons via multi-center delocalization within the polyindolic backbone.[13]

Eumelanins are the black-brown subgroup of melanins the natural nitrogen pigment for skin and hair pigmentation in mammals and widely diffused in animal kingdom.[14] In vivo the formation of eumelanins is the final outcome of oxidative metabolism of the aminoacids tyrosine (**Figure 1**), and in vitro a number of synthetic protocols have been developed to achieve these pigments by oxidative polymerization chiefly of the indolic precursors 5,6-dihidroxyndole (DHI) and its 2-carboxyl derivative (DHICA).[15]

View Article Online
DOI: 10.1039/D4MA00339J

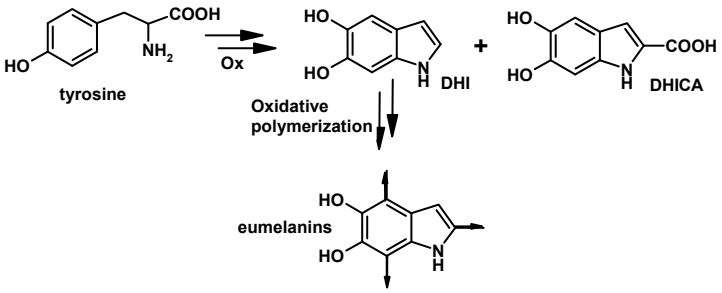

Figure 1. Schematic outline of early steps in eumelanin synthesis

Beyond its radical polymer nature melanin also exhibit other peculiar properties, form the broadband UV-vis absorption to the energy dissipating behavior and a mixed ionic/electronic semiconducting response toward charge transportation.[16 17] This last property firstly reported by and Procotr[18] is at the root of growing interest toward the exploitation of these pigments in organic electronics and, given their biocompatibility, bioelectronics.[19 20 21]Actually several application of eumelanin pigments and related materials as electroactive material have been reported in recent years including some studies addressing the integration of eumelanin pigment and PEDOT:PSS.[20] We recently proposed and systematically investigated the integration of commercial PEDOT:PSS (PH 1000) and eumelanin pigments prepared by oxidative polymerization of DHI and DHICA, to obtain respectively the two blends EuPH [22]and C-EuPH.[23] Key steps of the PH1000 - melanin blends are the dissolution of appropriate amounts of DHI and DHICA in the PH1000 commercial preparation; the deposition of the indole-added PH1000 by spin coating or drop casting; the melanization of the indole precursors by oxidative polymerization into the thin film solid layer.[21] The integration of eumelanins in the PH1000 produced a marked modification on the structural organization of the PEDOT and PSS chains[24] (chiefly) in the films likely connected with the conductivity properties of the blends, even allowing to fabricate an ITO free OLED.[22]

View Article Online
DOI: 10.1039/D4MA00339J

Capitalizing on this experience we addressed here the study of the Seebeck coefficient of EuPH blends in function of their EPR profiles eventually identifying a possible role of eumelanin pigment as radical dopant of PEDOT:PSS for thermoelectric applications.

Results.

EuPH thin films were fabricated basing on little modifications of a reported solid state protocol involving the preparation of DHI/PEDOT:PSS mixtures at different weight ratios. Key difference with respect to previously adopted procedures is in use of DMSO and not isopropyl alcohol to convey DHI in the PH1000. This choice was adopted to simplify the procedure where the doping effect of the DMSO was not relevant. Mixtures were use to fabricate thin films for chemical physical and electrical characterization. Drop casting and spin coating deposition were used to obtain the desired films featuring a thickness in the range of 200–500 nm. To permit straight characterization, the films were fabricated on quartz and glass substrates allowing the solid state ammonia-induced oxidative polymerization to run. Blends with DHI/PEDOT ratios of 25, 50 and 75%, respectively EuPH25, EuPH50 and EuPH75 were investigated and, for comparative purposes, films of sole DHI-eumelanin, and PH-1000 were also prepared (blanks).

Preliminary characterizations involved UV-vis and surface analysis to confirm the conversion of DHI to eumelanin and have information about the surface to contact for electrical measurements. In the panel a) of Figure 2 UV-vis profiles of EuPHs at the different weight ratios are reported together with the profiles of sole PH1000 and eumelanin for comparison purposes.

View Article Online
DOI: 10.1039/D4MA00339J

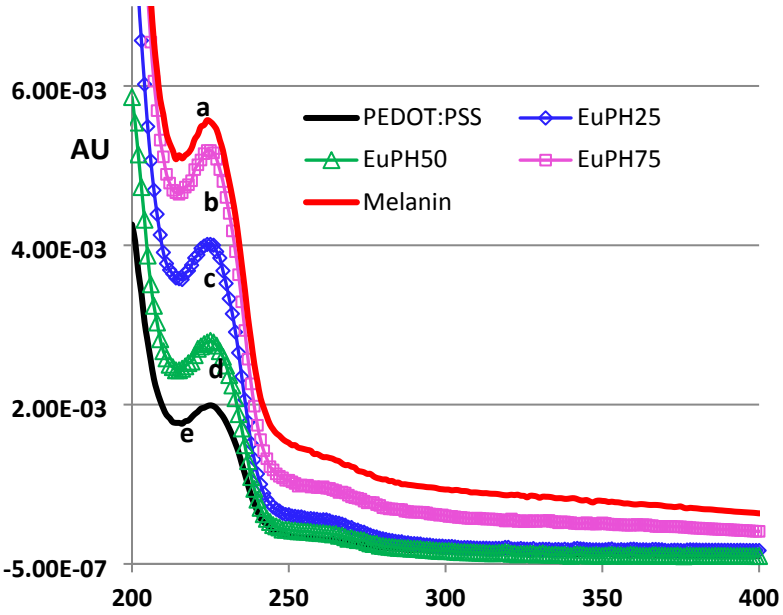

Figure 2 – UV spectra of (**a**) DHI-melanin, (**b**) EuPH75, (**c**) EuPH50, (**d**) EuPH25 and (**e**) treated PEDOT:PSS - thin films on quartz. Absorbances are normalized for the thickness

Surface analysis of the thin films was carried out by AFM for those samples intended for electrical measurements. The films were prepared by drop casting and inspected in tapping mode imaging to get both topographical and phase image(Figure S3). The films with low content of eumelanin exhibit a decrease of the surface roughness with respect to the sole PEDOT:PSS film or the sole Eumelanin film. No relevant roughness variation could be noted with eumelanin content variation.

For the thermoelectric property measurement a Linseis Thin Film Analyser system was used allowing both determination of the electrical conductivity σ and the Seebeck coefficients **S**. From the measurements of these quantities the thermo power $\mathbf{S}^2\sigma$ is also calculated to estimate the efficiency of the thermoelectric conversion. Details concerning the experimental procedure are reported in the SI, in brief thin films of blanks and blends onto a holder equipped with electrodes and temperature sensor.

View Article Online
DOI: 10.1039/D4MA00339J

In accordance with previous studies[22] the conductivity of the blends decreased with eumelanin content (**Figure3** top Panel) while the blanks values were 750 and 4.5x10e-5 siemens per centimeter for the sole PH1000 and DHI-melanin, respectively. At the same time the Seebeck coefficient showed an increase with eumelanin contented in those blends containing PH1000 although the growth profile does not follow eumelanin content but is asymptotic to the value of 23 µV/K in EuPH75. (Figure 3 top Panel)

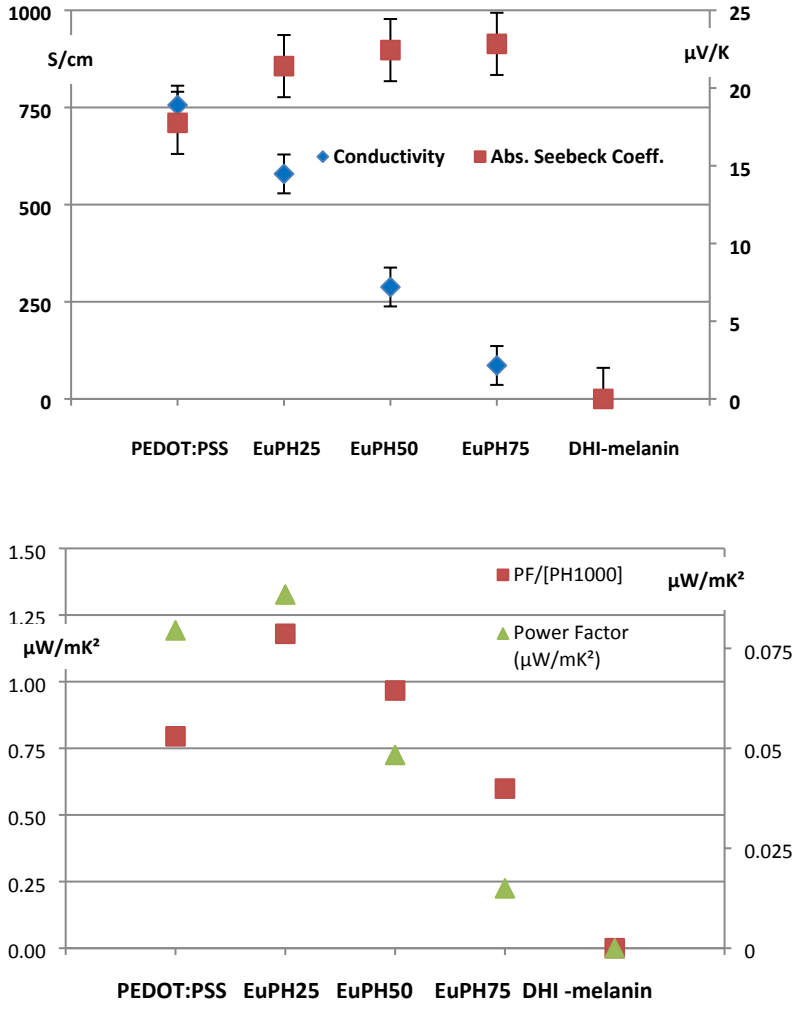

Figure 3. Top Panel: Seebeck (left axis) coefficient and conductivity (right axis); Bottom Panel: Power Factor (left axis) and Power Factor normalized to the PEDOT content (right axis).

View Article Online
DOI: 10.1039/D4MA00339J

To evaluate improvement of thermoelectric response of the blends the power factor (PF) is reported in function of eumelanin content showing an optimal value for the EuPH25 and, when PF is normalized on the PEDOT content, also the EuPH50 presented higher value than that of the sole PEDOT:PSS (**Figure 3** bottom Panel).

To investigate if and to what extent the properties discussed above are correlated to the configuration and delocalization of free electrons in the polymer molecules present in the samples, an EPR investigation was undertaken. The EPR spectrum of the PEDOT-PSS sample treated with ammonia vapors shows a broad singlet, arising from the quinoid configuration of the conjugated π-bond[25], at a g-value of 2.0023 ± 0.0002 corresponding to that of free electrons (**Figure 4**). The large peak-to-peak distance value (ΔB_{pp}) points to a statistical distribution of the radicals and to their wide delocalization[26] along. Lineshape analysis of this signal reveals an almost perfectly Lorentzian profile, which is ascribable to a predominating amorphous PEDOT phase.[27]. As already reported for PEDOT samples, the signal intensity increases with the microwave power with no evidence of saturation.[27]

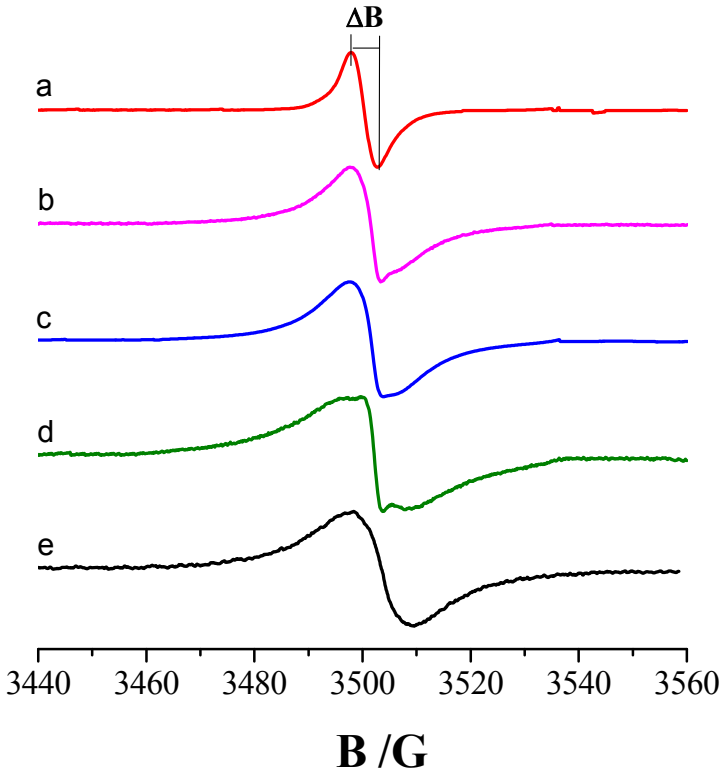

Figure 4. EPR spectra of (**a**) Melanin, (**b**) EuPH2/1, (**c**) EuPH1/1, (**d**) EuPH1/2 and (**e**) treated PEDOT:PSS.

View Article Online
DOI: 10.1039/D4MA00339J

On the other hand, the spectrum of the DHI melanin sample (Figure 4, a) shows a slightly asymmetric singlet at a relatively high g-value and equal to 2.0038 ± 0.0002, suggesting a contribution of the oxygens to spin delocalization. In this case, the lineshape is between the Lorentzian and Gaussian curves and suggests the presence of weakly interacting spin systems with weak exchange interactions.[28] With increasing the microwave power, the signal intensity reaches a maximum above which it slightly decreases.[29]

The spectra of the mixed samples (Figure 4, b-d) show the superposition of the signals due to the polymer and the melanin. Interestingly, the radical concentrations increase, thus indicating a synergistic effect between PEDOT and DHI melanin in radicals stabilization. Spectra analysis, performed using the Bruker Spinfit program, allows the estimation of the parameters reported in the Table 1. Interestingly, both PEDOT and DHI melanin signals in the mixed samples are narrower than those observed separately.

Table 1. Main relevant EPR parameters for EuPH blends in comparison with the starting components PH1000 and DHI-melanin. All samples with the exception of PH1000 no treatment were subjected to complete thin film fabrication protocol. PH1000 no treatment was obtained by same protocol but lacking the AISSP step.

Sample	**Radical concentration (spin/g)**	**g-factor**	**ΔB**	**Fraction of Gauss Function**
PH1000 no treatment	4.6E+17	2.0023	14.4	0
PH1000	6.9E+18	2.0023	12.1	0
EuPH25	8.7E+18	2.0023	11.0	0.1
		2.0038	3.8	0.6
EuPH50	1.7E+19	2.0023	10.6	0.1
		2.0038	3.5	0.5
EuPH75	6.1E+18	2,0023	10.8	0

View Article Online
DOI: 10.1039/D4MA00339J

		2.0038	4.0	0.4
DHI-melanin	1.8E+18	2.0038	4.9	0.4

Finally, in the power saturation curves (Figure 5) obtained by plotting the normalized peak amplitude (A/A_0) as function of the square root of the microwave power (P), the PEDOT contribution prevails and the curves show a monotonically increasing trend, which is completely different from that of pure DHI melanin proper of the free radical species with long relaxation times.

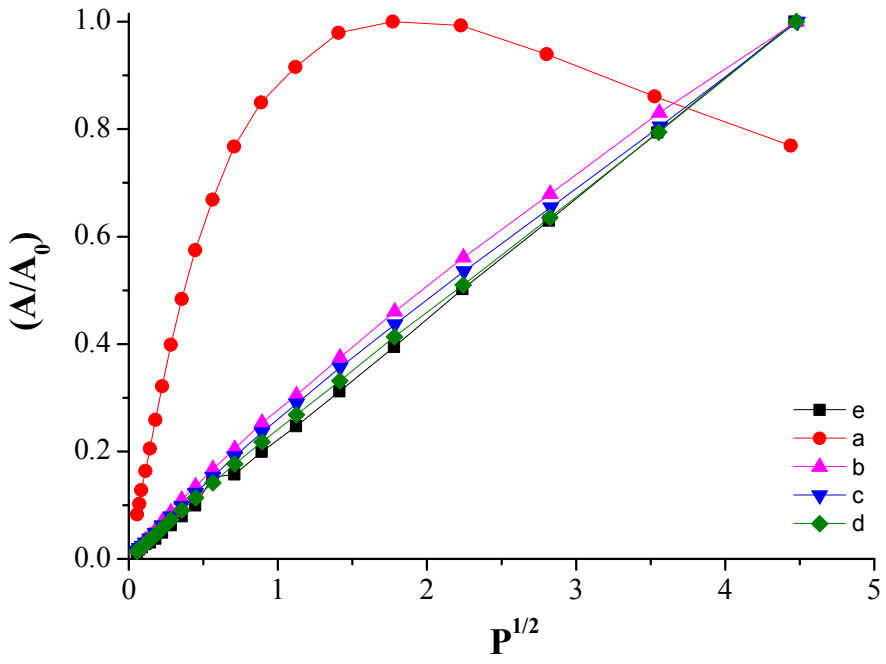

Figure 5. Power saturation curves corresponding to (**a**) Melanin, (**b**) EuPH2/1, (**c**) EuPH1/1, (**d**) EuPH1/2 and (**e**) treated PEDOT:PSS.

View Article Online
DOI: 10.1039/D4MA00339J

Discussion.

In order to investigate the possible exploitation of eumelanin for the thermopower improvement of PEDOT:PSS blends and the eventual link between the eumelanin radical content and the electrical properties of EuPHs we looked for correlations between electrical and EPR data of the blends at different relative eumelanin content moving from the analysis of sole eumelanin and PEDOT:PSS.

The EPR profile of the PEDOT:PSS is reported in several studied and is characterized by a large peak-to-peak distance value (ΔB_{pp}) because of the radicals and to their wide delocalization.[26] In EuPHs, after the introduction of eumelanin, the linewidth of EPR lines is influenced by the magnetic interactions between paramagnetic centers in the sample[25] resulting in a signal narrowing,[26] (**Figure 4**) likely ascribable to increased interactions decreasing the radical delocalization. It may be argued that ionic pairing between the positive charges of PEDOT and negative ones of phenoxy semiquinones within the eumelanin backbone can result in some obstacle to radical delocalization as radicals and ions in the polymers are linked in the pi system (**Figure 6**)

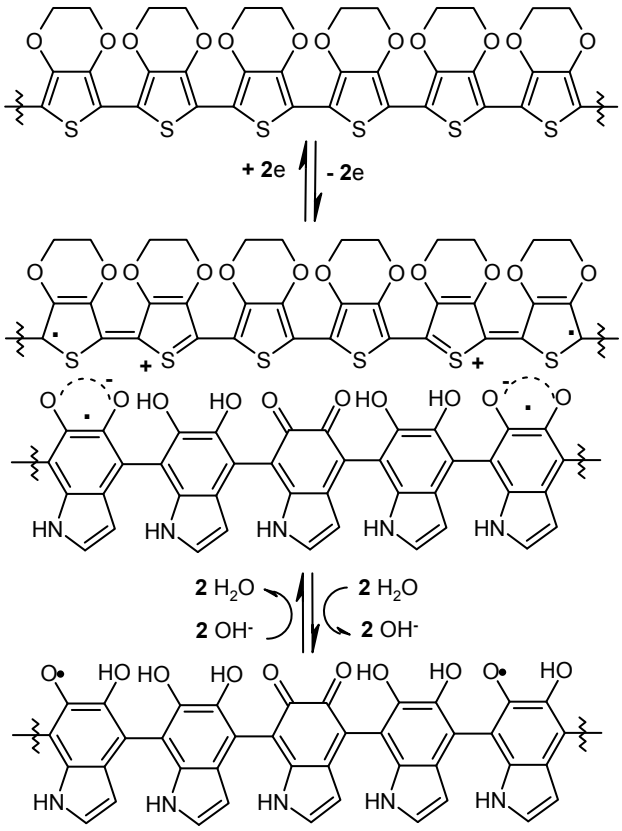

View Article Online
DOI: 10.1039/D4MA00339J

Figure 6. Schematic outline of possible interactions between PEDOT polarons and indolesemiquinone anions. Polarons generation after oxidative doping and semiquinone deprotonation after pH rising are represented.

This picture could also find some support by the observe little narrowing of the sole PEDOT signal after ammonia treatment step of the AISSP (**Figure S4**).

Notably, signal narrowing pairs with the increase of radical concentration (**Table 1**) a finding which further contribute to support the model of $PEDOT^{n+}$-$eumelanin^{m-}$ pairing. Indeed the (phenol + quinone)/semiquione equilibrium in eumelanin is pH sensitive[30] as the acidity of the penoxy form is increase with respects to the one of the phenol form (**Figure 7**).[31]

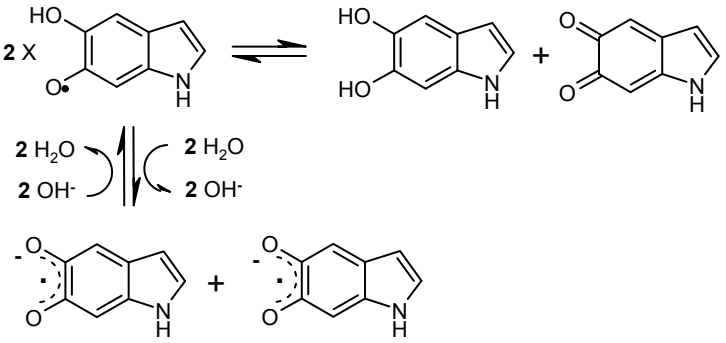

Figure 7. Indolesemiquinone redox equilibrium and pH depending ionization.

As the EuPH preparation protocol includes an exposition to ammonia vapors the consequent rise of the thin film pH shifts the redox equilibrium of the indole semiquinone toward the comproportionation and this results in turn in an increase of radical concentration in the semiquinone deprotonated anionic form.

Radicals in PEDOT are produced after the oxidative doping of the polymer (**Figure 6**), which is mandatory to achieve high conductivity levels,[32] and are considered associated to the formation of polarons whose

View Article Online
DOI: 10.1039/D4MA00339J

charge is to a degree stabilized by the anionic groups of PSS. This picture is partially modified by the introduction of eumelanin which is formed in situ after the polymerization of small DHI units dispersed in the PEDOT:PSS mixture, and thus intercalates between the PEDOT and the PSS according to X ray data from previous studies.[24] This intimate mixing is also supported here supported by the lack of relevant variations in the phase images of AFM allows to assume homogeneity of the film bulk properties. and suggests the effective and intimate mixing of the eumelanin and PEDOT:PSS components. thus supporting the affordability of macroscopic measurements/characteriyations of the films

Such proximity can be invoked in a possible model for the blending-induced increase of radical concentration. Indeed the positive charges of polarons can pair with the anionic conjugate base of radical semiquinone moieties into eumelanin polymers and in turn favour the redox comproportionation of catechol and quinone units.[30] This dynamic is similar to the pH induced quinone-indole comproportionation[30] but grounds not (or not only here) on the effect of ammonia basic nature while on the driving force provided by the charge pairing.

Both these effects are expected to operate in EuPHs as consequence of the chemical nature of the components and the fabrication protocol and can provide a solid model to justify the measured properties. Indeed, if we plot the radical concentration vs the ratio Seebeck/conductivity (**Figure 8**) we can see some trend similarities suggesting possible direct contribution of eumelanin doping of PEDOT thermoelectrical properties.

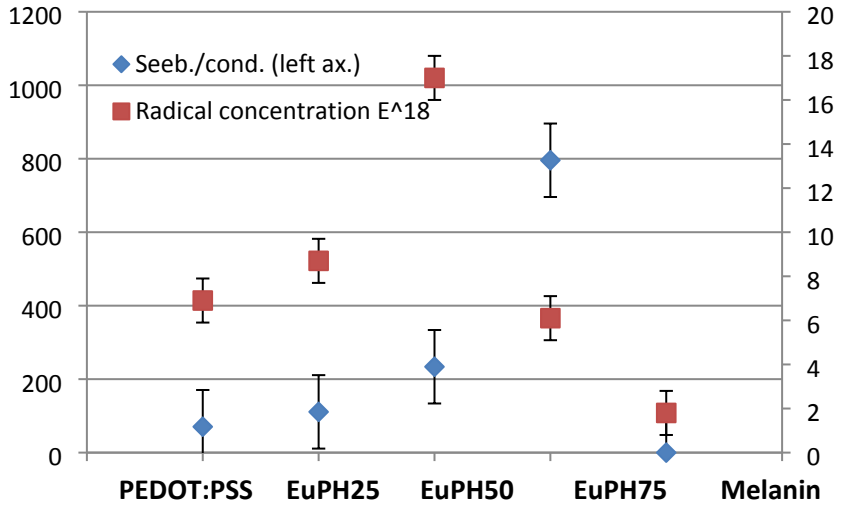

Figure 8. Seebeck over conductivity ratio (left axis) and radical concentration.

View Article Online
DOI: 10.1039/D4MA00339J

Conclusion.

The chemical characteristic of semiquinone moieties within the eumelanin backbone allowed to expand the literature application cases of radical species for thermopower enhancement of conducting polymers. The pH dependence of semiquinone redox equilibrium combined with the acidity of semiquinone resulted in a synergistic increase of radical concentration in EuPH blends a parameter which appears to correlated with the Seebeck coefficient and the improvement of PEDOT thermopower.

Although more systematic investigations have to be designed and carried out before a quantitative model can be defined, this study disclosed how eumelanin can play a role in the modulation of Seebeck coefficient vs conductivity in PEDOT-based conductive materials and opens an entire new scenario for the application of a natural biocompatible product in organic electronics for energy conversion.

Experimental.

More details concerning materials and methods are reported in the Supporting Information

Film preparation and EPR measurements:

The EuPH thin films were fabricated by spin coating of the appropriate mother solution containing DHI and PH1000. DHI/(PEDOT:PSS) ratios of 0.25/(1:2.5), 0.5/(1:2.5) and 0.75/(1:2.5),w/w), were obtained by mixing two mother solutions: a) DHI in isopropyl alcohol (8 mg/mL) and b) PEDOT:PSS in water (a Clevios™ PH 1000 commercial product featuring 1÷1.3 % weight content of polymers, with a PEDOT: PSS ratio of 1:2.5).[33] In order to enhance the conductivity of the pristine PEDOT:PSS, 5% DMSO was added to the PH 1000.[33] Before use the solutions were vortex mixed under oxygen free atmosphere, filtered through a 0.45 µm Whatman membrane and spin coated on quartz substrates using a Laurell WS-650MZ-23NPP/LITE spin coater. After drying and annilation (80°C for 10'on a hot plate in air), the resulting films thickness, measured by a KLA Tencor P-10 surface profiler, were in the range 100-150 nm. Once prepred the layers was then subjected to the ammonia-induced solid state polymerization (AISSP) protocol *rif(50) to finally obtain the desired EuPH thin film, by exposing the DHI-PEDOT:PSS films for 1 h to air-equilibrated gaseous ammonia from an ammonia solution (28% in water) inside a sealed chamber at 1 atm pressure and at controlled temperature (25°C÷ 40°C).

View Article Online
DOI: 10.1039/D4MA00339J

EPR measurements were conducted using a Bruker Elexys E-500 spectrometer that was equipped with a highly sensitive probe head. The samples were placed in flame-sealed glass capillaries, which were then inserted into a standard 4 mm quartz sample tube. The measurements took place at room temperature with specific instrumental settings: a sweep width of 140 G, resolution of 1024 points, modulation amplitude of 1.0 G, conversion time of 20.5 ms, and a time constant of 10.24 ms. The field modulation amplitude was carefully adjusted to prevent signal overmodulation. Scans and microwave power were optimized to avoid saturation of the resonance absorption curve. In power saturation experiments, the microwave power was gradually increased from 0.001 to 127 mW. The signal line width, known as ΔB, was calculated as the peak-to-peak distance of the first-derivative signal, while the g-factor and spin-concentration parameters were determined using an internal standard, such as Mn^{2+}-doped MgO, which was introduced into the quartz tube alongside each sample[34 35] Due to uncontrolled sample hydration during measurements, spin concentration values were considered as rough estimates. A 10% error in radical concentration was attributed to sample positioning, while a g-factor error of approximately 3×10^4 was associated with line-width.

Acknowledgments

Financial support from ENEA (Italian Project RdS_PTR22-24), PNRR projetc Pathogen Readiness Platform for CERIC-ERIC Upgrade, PNRR NEST - Network 4 Energy Sustainable Transition.

References.

1. A. Khasbaatar, Z. Xu, J.-H. Lee, G. Campillo-Alvarado, C. Hwang, B. N. Onusaitis and Y. Diao, *Chemical Reviews*, 2023, **123**, 8395-8487.
2. P. Sang, Q. Chen, D.-Y. Wang, W. Guo and Y. Fu, *Chemical Reviews*, 2023, **123**, 1262-1326.
3. A. Koklu, D. Ohayon, S. Wustoni, V. Druet, A. Saleh and S. Inal, *Chemical Reviews*, 2022, **122**, 4581-4635.
4. M. Wu, K. Yao, D. Li, X. Huang, Y. Liu, L. Wang, E. Song, J. Yu and X. Yu, *Materials Today Energy*, 2021, **21**, 100786.
5. Z. Yan, S. Luo, Q. Li, Z.-S. Wu and S. Liu, *Advanced Science*, 2024, **11**, 2302172.
6. X. Dai, Q. Meng, F. Zhang, Y. Zou, C.-a. Di and D. Zhu, *Journal of Energy Chemistry*, 2021, **62**, 204-219.
7. M. Massetti, F. Jiao, A. J. Ferguson, D. Zhao, K. Wijeratne, A. Wurger, J. L. Blackburn, X. Crispin and S. Fabiano, *Chem. Rev.*, 2021, **121**, 12465-12547.
8. J. Hurtado-Gallego, S. Sangtarash, R. Davidson, L. Rincón-García, A. Daaoub, G. Rubio-Bollinger, C. J. Lambert, V. S. Oganesyan, M. R. Bryce, N. Agraït and H. Sadeghi, *Nano Letters*, 2022, **22**, 948-953.

View Article Online
DOI: 10.1039/D4MA00339J

9. Y. Joo, L. Huang, N. Eedugurala, A. E. London, A. Kumar, B. M. Wong, B. W. Boudouris and J. D. Azoulay, *Macromolecules*, 2018, **51**, 3886-3894.
10. E. P. Tomlinson, M. J. Willmore, X. Zhu, S. W. A. Hilsmier and B. W. Boudouris, *ACS Applied Materials & Interfaces*, 2015, **7**, 18195-18200.
11. M. D'Ischia, A. Napolitano, A. Pezzella, P. Meredith and T. Sarna, *Angewandte Chemie - International Edition*, 2009, **48**, 3914-3921.
12. J. V. Paulin, A. Batagin-Neto and C. F. O. Graeff, *The Journal of Physical Chemistry B*, 2019, **123**, 1248-1255.
13. P. Manini, V. Lino, G. D'Errico, S. Reale, A. Napolitano, F. De Angelis and M. d'Ischia, *Polymer Chemistry*, 2020, **11**, 5005-5010.
14. M. D'Ischia, K. Wakamatsu, A. Napolitano, S. Briganti, J. C. Garcia-Borron, D. Kovacs, P. Meredith, A. Pezzella, M. Picardo, T. Sarna, J. D. Simon and S. Ito, *Pigment Cell and Melanoma Research*, 2013, **26**, 616-633.
15. M. d'Ischia, A. Napolitano, A. Pezzella, P. Meredith and M. Buehler, *Angewandte Chemie - International Edition*, 2020, **59**, 11196-11205.
16. J. V. Paulin, S. Bayram, C. F. O. Graeff and C. C. B. Bufon, *ACS Applied Bio Materials*, 2023, **6**, 3633-3637.
17. A. B. Mostert, B. J. Powell, F. L. Pratt, G. R. Hanson, T. Sarna, I. R. Gentle and P. Meredith, *Proceedings of the National Academy of Sciences*, 2012, **109**, 8943-8947.
18. J. McGinness, P. Corry and P. Proctor, *Science*, 1974, **183**, 853-855.
19. M. Sheliakina, A. B. Mostert and P. Meredith, *Materials Horizons*, 2018, **5**, 256-263.
20. N. L. Nozella, J. V. M. Lima, R. F. de Oliveira and C. F. d. O. Graeff, *Materials Advances*, 2023, **4**, 4732-4743.
21. A. Pezzella, M. Barra, A. Musto, A. Navarra, M. Alfè, P. Manini, S. Parisi, A. Cassinese, V. Criscuolo and M. D'Ischia, *Materials Horizons*, 2015, **2**, 212-220.
22. L. Migliaccio, S. Aprano, L. Iannuzzi, M. G. Maglione, P. Tassini, C. Minarini, P. Manini and A. Pezzella, *Advanced Electronic Materials*, 2017, **3**.
23. L. Migliaccio, F. Gesuele, P. Manini, M. G. Maglione, P. Tassini and A. Pezzella, *Materials*, 2020, **13**.
24. L. Migliaccio, D. Altamura, F. Scattarella, C. Giannini, P. Manini, F. Gesuele, M. G. Maglione, P. Tassini and A. Pezzella, *Advanced Electronic Materials*, 2019, **5**.
25. A. Zykwinska, W. Domagala and M. Lapkowski, *Electrochemistry Communications*, 2003, **5**, 603-608.
26. A. k. Anbalagan, S. Gupta, M. Chaudhary, R. R. Kumar, Y.-L. Chueh, N.-H. Tai and C.-H. Lee, *RSC Advances*, 2021, **11**, 20752-20759.
27. W. Domagala, B. Pilawa and M. Lapkowski, *Electrochimica Acta*, 2008, **53**, 4580-4590.
28. L. Panzella, G. Gentile, G. D'Errico, N. F. Della Vecchia, M. E. Errico, A. Napolitano, C. Carfagna and M. d'Ischia, *Angewandte Chemie International Edition*, 2013, **52**, 12684-12687.
29. L. Panzella, G. D'Errico, G. Vitiello, M. Perfetti, M. L. Alfieri, A. Napolitano and M. d'Ischia, *Chemical Communications*, 2018, **54**, 9426-9429.
30. S.-S. Chio, J. S. Hyde and R. C. Sealy, *Archives of Biochemistry and Biophysics*, 1982, **215**, 100-106.
31. A. Pezzella, O. Crescenzi, L. Panzella, A. Napolitano, E. J. Land, V. Barone and M. d'Ischia, *Journal of the American Chemical Society*, 2013, **135**, 12142-12149.
32. I. Zozoulenko, A. Singh, S. K. Singh, V. Gueskine, X. Crispin and M. Berggren, *ACS Applied Polymer Materials*, 2019, **1**, 83-94.
33. Y. Xia and J. Ouyang, *ACS Applied Materials and Interfaces*, 2012, **4**, 4131-4140.

View Article Online
DOI: 10.1039/D4MA00339J

34. F. Amantea, G. Antignani, G. Pota, E. Cascone, S. Parisi, M. Alfè, V. Gargiulo, G. Luciani, A. Pezzella, G. D'Errico, R. Di Capua and G. Vitiello, *Applied Surface Science*, 2023, **633**, 157608.
35. F. Furlani, G. Pota, A. Rossi, G. Luciani, E. Campodoni, F. Mocerino, G. D'Errico, A. Pezzella, S. Panseri, G. Vitiello and M. Sandri, *Colloids and Surfaces B: Biointerfaces*, 2024, **235**, 113756.

View Article Online
DOI: 10.1039/D4MA00339J

UNIVERSITY of NAPLES FEDERICO II
DEPARTMENT OF PHYSICS "*Ettore Pancini*"
Prof. Alessandro Pezzella

Naples
June 25, 2024

Dear Editor,

The data supporting this article have been included as part of the Supplementary Information.

Sincerely,
Alessandro Pezzella, PhD

View Article Online
DOI: 10.1039/D4MA00339J

Via Cintia, Complesso universitario di Monte Sant'Angelo, Building n. 6 – 80126 - Naples - ITALY
Room 2Ma18; Tel. 081 674130; e-mail: alessandro.pezzella@unina.it;
https://www.docenti.unina.it/alessandro.pezzella